New Vortex-Matter Size Effect Observed in $Bi_2Sr_2CaCu_2O_{8+\delta}$

Y. M. Wang, M. S. Fuhrer, and A. Zettl*
Department of Physics, University of California at Berkeley, Berkeley, California 94720
and Materials Sciences Division, Lawrence Berkeley National Laboratory, Berkeley, California 94720

S. Ooi and T. Tamegai
Department of Applied Physics, The University of Tokyo, Hongo, Bunkyo-ku, Tokyo 113-8656 Japan
(Received 24 October 2000)

The vortex-matter 3D to 2D phase transition is studied in micron-sized $Bi_2Sr_2CaCu_2O_{8+\delta}$ single crystals using local Hall magnetization measurements. At a given temperature, the second magnetization peak, the signature of a possible 3D–2D vortex phase transition, disappears for samples smaller than a critical length. We suggest that this critical length should be equated with the 2D vortex lattice ab-plane correlation length R_c^{2D}. The magnitude and temperature dependence of R_c^{2D} agree well with Larkin-Ovchinnikov collective pinning theory.

DOI: 10.1103/PhysRevLett.86.3626 PACS numbers: 74.60.Ge, 74.25.Dw, 74.90.+n

Vortex matter, comprising the vortices in the mixed state of a high T_c superconductor, is considered a model system for the study of phase transitions. The competition between three important energy scales (vortex-vortex interaction, pinning, and thermal) gives rise to a rich vortex-matter phase diagram. At high temperature, thermal energy causes vortex lattice melting [1], while at low temperature, pinning can drive a transition of the vortex solid in layered anisotropic superconductors in which a three-dimensional (3D) vortex line lattice dissociates into two-dimensional (2D) vortex pancakes with mainly ab-plane correlation [2–4]. The relevant parameters which determine the state of vortex-matter, temperature, and applied magnetic field (analogous to pressure in atomic matter) may each be varied independently over several orders of magnitude. In addition, the effects of tuning a wide range of materials parameters have been studied, such as disorder type and strength, anisotropy, and doping level. However, the effects of finite sample size on the state of vortex matter have received relatively little attention [5,6]. Size effects, which have been important in the study of atomic matter phase transitions [7,8], should also provide useful insight in the study of vortex matter. In addition, the richness of the vortex-matter phase diagram offers the possibility of studying new size effects which have no atomic matter analogs.

In this Letter, we investigate the effect of greatly reduced sample size on the disorder-driven 3D–2D vortex transition in $Bi_2Sr_2CaCu_2O_{8+\delta}$ (BSCCO). At low fixed temperatures, we find through local magnetization measurements that the second magnetization peak (SMP), the signature of a possible vortex solid 3D–2D transition [9], disappears for samples smaller than a temperature-dependent critical length. We suggest that the observed critical length R_{cr} reflects the 2D vortex lattice ab-plane correlation length R_c^{2D}. For samples smaller than R_c^{2D}, the vortex lattice becomes insensitive to the disorder potential, and the disorder-driven vortex 3D–2D phase transition is absent. The magnitude and temperature dependence of R_{cr} agree with R_c^{2D} in the Larkin-Ovchinnikov collective pinning model [10].

Single crystals of BSCCO were grown using the floating zone method [11]. The crystals were cleaved into 10 and 4.5 μm thick pieces. Disks and squares of lateral dimensions ranging from diameter $D = 30$ to 180 μm were then microfabricated from these pieces using photolithography and Ar ionmilling (fabrication details will be reported in a later publication [12]). The samples were slightly overdoped ($T_c = 87$ K) after the fabrication by annealing in air at 550 °C for 20 hours. The local magnetization of the samples was determined by placing the samples in a superconducting solenoid with the applied field H_a parallel to the crystal c axis. All local magnetization measurements were taken at the face center of the sample using a microfabricated GaAs/AlGaAs Hall sensor [1]. Figure 1 shows a scanning electron microscopy image of [1(a)] the bare GaAs/AlGaAs Hall sensor and [1(b)] with a BSCCO disk mounted in place on the sensor. Local magnetization measurements on zero-field-cooled samples were made at a magnetic field ramp rate of 1 G/s.

Figure 2 compares the local magnetization, $B_z - H_a$, vs B_z for two different size BSCCO disks at two selected

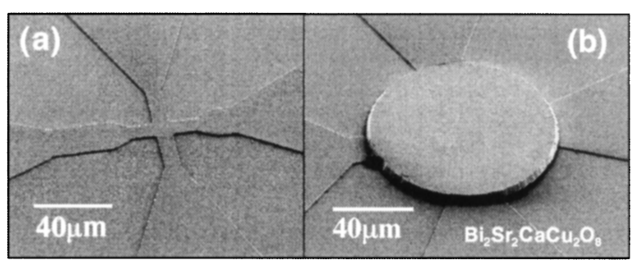

FIG. 1. Scanning electron microscope image of a GaAs/AlGaAs Hall sensor (a) with no sample and (b) with a BSCCO disk mounted on top of the Hall sensor. The sensor has an active area of 10×10 μm^2. The BSCCO disk has a diameter of 93 μm and a thickness of 4.5 μm.

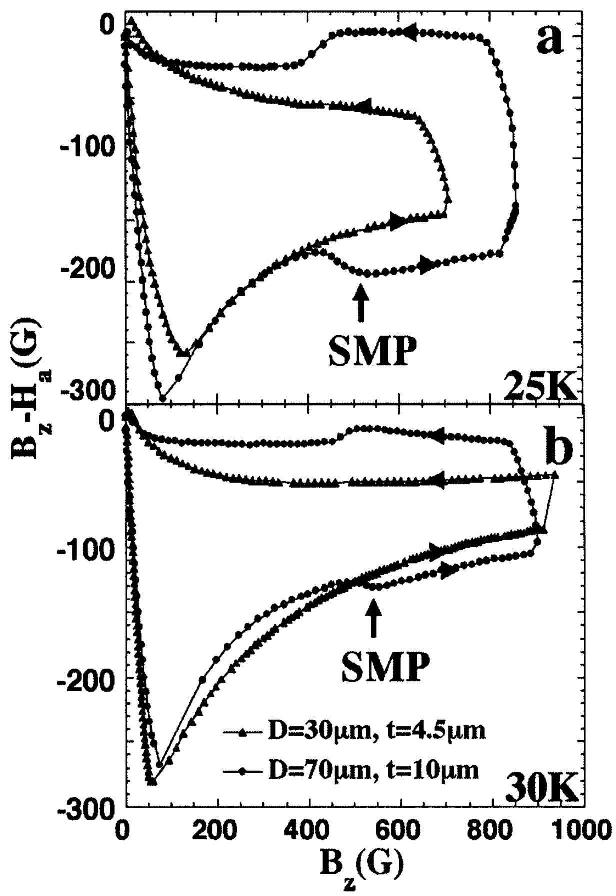

FIG. 2. Local magnetization curves, $B_z - H_a$ vs magnetic induction B_z at (a) 25 K and (b) 30 K for BSCCO disks with identical thickness-to-diameter ratio of $t/D \approx 0.15$. The two disks have diameters of 70 μm (•) and 30 μm (△), and thickness of 10 μm and 4.5 μm, respectively. The arrow-head indicates the ramp direction of the applied field H_a. The SMP, as indicated by an arrow in (a) and (b) for the 70 μm disk, is absent in the 30 μm disk at both temperatures.

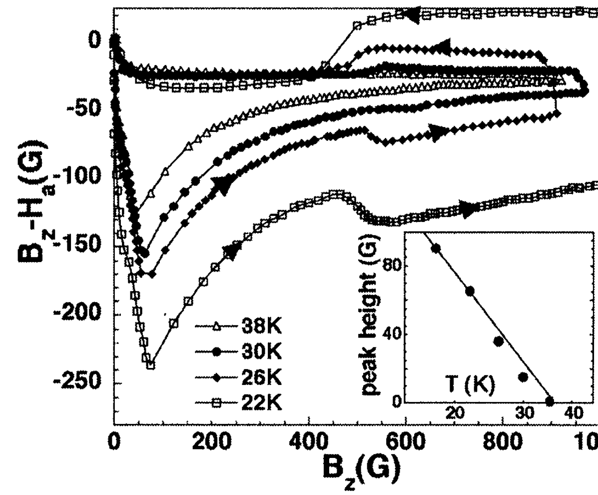

FIG. 3. $B_z - H_a$ vs B_z for a 90 μm square at selected temperatures. The inset shows the SMP peak height as a function of temperature on a logarithmic scale. Extrapolation of the peak height to zero defines the critical temperature T_{cr} below which the SMP is observed.

temperatures, 25 and 30 K. H_a is the applied field parallel to the c axis of BSCCO, and B_z is the local magnetic induction as determined by the Hall sensor. The two disks have diameters D of 70 and 30 μm, and thickness t of 10 and 4.5 μm, respectively. The most striking feature of Fig. 2 is that the SMP, as denoted by the arrow at $\approx$550 G in the 70 μm disk data, is absent in the 30 μm disk at both temperatures. From Fig. 2 we infer that at both 30 and 25 K the critical lateral size R_{cr} at which the SMP disappears lies somewhere between 70 and 30 μm.

In order to determine accurately $R_{cr}(T)$, magnetization measurements for a given sample were repeated at a series of fixed temperatures. Figure 3 shows representative data for a different BSCCO sample, in this case a 90 μm square with $t = 10$ μm. For this sample the SMP is observed only at temperatures somewhat below 38 K, again at a temperature independent B_z of 550 G. B_z is consistent with the previously published SMP field B_z of macroscopic overdoped BSCCO samples [13]. We thus find that, when the SMP is observed at all in small BSCCO samples, it occurs at the same magnetic induction as that for larger samples. Figure 3 shows that, as the temperature is increased, the SMP anomaly becomes successively smaller. Above a (sample-size dependent) critical temperature T_{cr}, the SMP disappears completely. In order to determine T_{cr} accurately, we plot the SMP peak height (defined as the difference of the local hysteretic magnetization for magnetic induction just before and just after the SMP anomaly) as a function of temperature, as shown in the inset of Fig. 3. The peak height can be fit empirically with a logarithmic temperature dependence indicating an abrupt trend to zero height at finite temperature. Extrapolation of the peak height to zero defines T_{cr}. For the 90 μm sample of Fig. 3, the SMP disappears definitively at 35 K. Hence, $R_{cr}(T = 35\text{ K}) = 90$ μm.

We have repeated the measurements of Fig. 3 for eight different samples of different size ranging from 30 to 180 μm, thus generally determining $T_{cr}(R)$, or equivalently, $R_{cr}(T)$. Figure 4 shows the results, which define a new SMP phase diagram for BSCCO incorporating sample size. The temperature interval plotted is 20 to 45 K, which is the relevant temperature interval for the SMP using local magnetization measurement [13]. We find no appreciable difference in the phase diagram between circular and square samples.

We now discuss these results more fully. We first consider the expected geometry dependence of the various contributions to the total (measured) hysteretic magnetization. There are two mechanisms which give rise to hysteresis in the magnetization: one is bulk impurity pinning [14], which represents pinning of vortices by point disorder in the bulk of the sample; the other is surface barriers, which include the Bean-Livingston surface barrier [15] and geometrical barriers [16,17]. The total local magnetization hysteresis is the sum of bulk pinning hysteresis

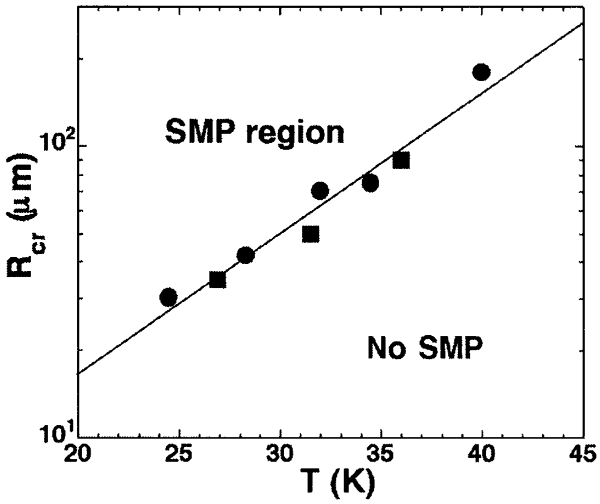

FIG. 4. Critical sample size $R_{cr}(T)$ below which the SMP is absent, shown as a function of temperature. All samples used for this plot are 10 μm thick. R_{cr} represents the diameter for a disk and the width for a square. Filled squares and circles represent measurements on square and circular samples, respectively. The line is a fit to the Larkin-Ovchinnikov ab-plane vortex correlation length $R_{cr} = (1.8\ \mu\text{m})\exp(T/9\ \text{K})$.

$M_{\text{bulk}}(B_z)$ and surface barrier hysteresis $M_{\text{barrier}}(B_z)$ [18], where $M_{\text{bulk}}(B_z) = |(B_z - H_a)\uparrow - (B_z - H_a)\downarrow|$ with $\uparrow$ and $\downarrow$ representing ascending and descending field directions, respectively. Each pinning mechanism is expected to have a different dependence on sample dimension: $M_{\text{bulk}} \propto DJ_c$ according to the Bean model [14], where J_c is the critical current density and D the sample diameter; and M_{barrier} is expected to be a function of the thickness-to-diameter ratio t/D for both Bean-Livingston surface barrier and geometrical barrier [17–21]. Because M_{barrier} increases and M_{bulk} decreases as D decreases, the barrier magnetization overwhelms bulk magnetization in small samples [22]. While the continuity of M_{barrier} at the 3D–2D transition remains unclear [23], ideally, samples of similar M_{barrier} should be studied such that differences in M_{bulk} would be evident.

For Fig. 2 we have in fact carefully chosen samples of similar thickness-to-diameter ratios ($t/D \sim 0.15$ for both samples) in order to achieve a similar value of M_{barrier}. Confirming the theoretical prediction, the vortex penetration field H_p, defined as the value of H_a at the first negative peak of the local magnetization, $H_a = B_z - (B_z - H_a)$, is indeed identical for both disks (with values $H_p \approx 380$ G at 25 K and 330 G at 30 K). Thus these two samples have the same value of M_{barrier} above H_p, and the total hysteretic magnetization difference between the two disks is strictly the difference in the bulk pinning magnetization—surface effects have been eliminated. It is thus instructive to further compare the magnetization data of these two samples, as seen in Fig. 2.

Below the SMP, the total magnetization, and thus M_{bulk}, is narrower in the 30 μm disk, in agreement with the Bean model [14] where $M_{\text{bulk}} \propto DJ_c$. The 70 μm disk has a magnetization jump at $B_z \approx 550$ G, indicating a 3D–2D phase transition (not observed in the 30 μm disk). It is believed that across the SMP line of the vortex phase diagram, a 3D vortex-line solid dissociates into a randomly pinned pancake vortex solid. As the pancake vortex solid, with its smaller correlated volume [10], can better adapt to the random pinning centers, the critical current increases upon the transition from the 3D to the 2D state. The SMP signifies the increase of critical current since $M_{\text{bulk}} \propto DJ_c$. We expect that, if the vortex 3D–2D transition exists in the 30 μm disk, the increase in J_c should be the same as in the 70 μm disk, and a magnetization peak of approximately 3/7 (30 μm/70 μm) the magnitude of that in the 70 μm disk should be observed. This is inconsistent with our observations. The absence of an observed peak in the 30 μm disk at temperatures higher than 25 K (Fig. 2) allows us to put an upper bound on the peak height of at least 10 times smaller than this estimate, indicating a dramatic suppression of the critical current increase associated with rearrangement of vortices at the 3D–2D transition. We can draw similar conclusions for our other sample sets.

What is the physical origin of the shrinking of the SMP line in very small BSCCO samples? Kopelevich and Esquinazi recently proposed vortex avalanches as a source of the SMP in BSCCO [5]. Their model suggests that in bulk BSCCO the heat generated by vortex motion cannot be dissipated fast enough due to the large lateral sample size. Sample heating lowers the energy barrier for vortex influx, which results in the SMP. In small samples, heat is released faster than its generation rate due to the short lateral dimension, and therefore the SMP may be absent. Unfortunately, this model predicts [5] a temperature dependence of R_{cr} at odds with our findings in Fig. 4.

Another possibility is that the shrinking of the SMP line in small samples is a result of a sample-size-induced overall downward shift in temperature of the vortex lattice *melting* line and its associated critical end point. This is relevant since in BSCCO the vortex solid SMP line is connected to the vortex lattice melting transition line by the critical end point [1]. Since at $B_z \approx 550$ G the ratio of the number of edge vortices to the bulk vortices reaches $\sim$3% in the 30 μm disk, the phase transition in consideration may no longer be in the thermodynamic regime. If vortex lattice melting were indeed affected by the large surface-to-volume ratio of small samples (as in atomic matter melting), there could result a compression of the SMP line at low temperatures. We have tested this hypothesis by independently examining the sample size dependence of the vortex lattice melting line. Above $T = 60$ K, the melting onset field B_z (melting) and the magnitude of the melting jumps are independent of sample size and agree with reported results on overdoped BSCCO [13,24]. Thus, an overall downward shift of the melting line is ruled out as the origin of the shifting of the SMP.

We propose here a new model that accounts naturally for the SMP disappearance above T_{cr} in small samples. The SMP signifies an increase in bulk vortex pinning, and, hence, an increase in J_c, as the vortex lattice structure changes from 3D, with primarily out-of-plane vortex correlation, to 2D, with primarily in-plane vortex correlation. In the Larkin-Ovchinnikov (LO) collective pinning model, the vortex lattice is treated as correlated within a volume defined by the ab-plane correlation length R_c, and the c-axis correlation length L_c. The vortex lattice may rearrange to lower its energy in the pinning potential only on scales larger than the correlation volume. Upon the conventional 3D to 2D transition, L_c decreases, while R_c increases. The net effect is an increase in the pinning energy of the 2D state, which favors its formation. However, the LO model should break down for samples with one or more dimensions smaller than the relevant correlation lengths.

In our samples for certain temperatures the lateral sample dimension becomes smaller than the 2D ab-plane correlation length R_c^{2D}. In this case, the 2D vortex lattice in each superconducting layer is correlated across the entire sample. The ability of the vortex lattice to rearrange in response to the disorder potential is reduced, and, hence, the 2D state becomes less favorable energetically. Hence, we expect a suppression of the 2D phase in samples smaller than the 2D ab-plane correlation length R_c^{2D}.

Our model may be tested quantitatively. We estimate the magnitude and temperature dependence of R_c^{2D} using the 2D LO collective pinning model [10,25] in order to make comparison with the experimentally determined $R_{cr}(T)$. In the 2D LO collective pinning model the out-of-plane pancake vortex correlation length is taken as the interlayer distance, and the ab-plane correlation length is given as

$$R_c^{2D} = \sqrt{\frac{C_{66} c}{J_c B_z \xi}}\, a_o\,, \tag{1}$$

where the shear modulus of the vortex lattice $C_{66} \approx B_z H_{c1}/16\pi$, the critical current $J_c(T) \approx J_c(0) \times \exp(-T/T_o)$ [20], ξ is the ab-plane coherence length, c is the speed of light, and the inter-vortex distance $a_o = \sqrt{\Phi_0/B_z}$, with Φ_0 the superconducting flux quantum. The temperature dependence of R_c^{2D} comes primarily from the exponential temperature dependence of the critical current J_c; thus we expect an exponential dependence of R_c^{2D} on temperature. If we assume reasonable values of $\xi = 2.5$ nm, $H_{c1} = 100$ G [26], and $J_c(0) = 5 \times 10^5$ A/cm^2 [25], we find $R_c = (2.2\ \mu\text{m})\exp(T/2T_o)$ at $B_z = 550$ G, where T_o is the temperature exponent of the critical current, estimated to be of order 10 K in BSCCO.

The solid line in Fig. 4 is a fit of Eq. (1) to the experimental data, yielding $R_{cr} = (1.8\ \mu\text{m})\exp(T/9\text{ K})$. The exponential temperature dependence agrees with the expected behavior of R_c^{2D}, giving a reasonable $T_o = 4.5$ K for the critical current temperature exponent. The agreement in the prefactor is excellent, given the uncertainty in H_{c1} and $J_c(0)$.

We thank Aaron Lindenberg for helpful interactions. This research was supported in part by NSF Grants No. DMR-9801738 and No. DMR-9501156, by the Director, Office of Energy Research, Office of Basic Energy Sciences, Materials Sciences Division of the U.S. Department of Energy under Contract No. DEAC03-76SF00098, and by CREST and Grant-in-Aid for Scientific Research from the Ministry of Education, Science, Sports and Culture of Japan.

*Corresponding author.

[1] E. Zeldov *et al.,* Nature (London) **375**, 373 (1995).
[2] T. Tamegai *et al.,* Physica (Amsterdam) **213C**, 33 (1993).
[3] R. Cubitt *et al.,* Nature (London) **365**, 407 (1993).
[4] T. Giamarchi and P. Le Doussal, Phys. Rev. B **55**, 6577 (1997).
[5] Y. Kopelevich and P. Esquinazi, J. Low Temp. Phys. **113**, 1 (1998).
[6] R. Wördenweber and P.H. Kes, Phys. Rev. B **34**, 494 (1986).
[7] R.S. Berry, Nature (London) **393**, 212 (1998).
[8] A.N. Goldstein, C.M. Echer, and A.P. Alivisatos, Science **256**, 1425 (1992).
[9] Various models other than vortex solid 3D–2D transition have been proposed to explain the SMP in BSCCO, including onset of vortex entanglement [M.F. Goffman *et al.,* Phys. Rev. B **57**, 3663 (1998)]; and order-disorder phase transitions [Jan Kierfeld and Valerii Vinokur, Phys. Rev. B **61**, 14 928 (2000)]. In the rest of our discussion the term "vortex solid 3D–2D phase transition" is used to collectively represent also these models for the SMP, the signature of a vortex-solid structural phase transition.
[10] A.I. Larkin and Yu.N. Ovchinnikov, J. Low Temp. Phys. **34**, 409 (1979).
[11] S. Ooi, T. Shibauchi, and T. Tamegai, Physica (Amsterdam) **302C**, 339 (1998).
[12] Y.M. Wang *et al.* (to be published).
[13] B. Khaykovich *et al.,* Phys. Rev. Lett. **76**, 2555 (1996).
[14] C.P. Bean, Phys. Rev. Lett. **8**, 250 (1962).
[15] C.P. Bean and J.D. Livingston, Phys. Rev. Lett. **12**, 14 (1964).
[16] E. Zeldov *et al.,* Phys. Rev. Lett. **73**, 1428 (1994).
[17] Th. Schuster *et al.,* Phys. Rev. Lett. **73**, 1424 (1994).
[18] L. Burlachkov, Phys. Rev. B **47**, 8056 (1993).
[19] E.H. Brandt, Phys. Rev. B **60**, 11 939 (1999).
[20] A.V. Kuznetsov, D.V. Eremenko, and V.N. Trofimov, Phys. Rev. B **56**, 9064 (1997).
[21] L. Burlachkov *et al.,* Phys. Rev. B **50**, 16 770 (1994).
[22] Y.M. Wang *et al.,* Physica (Amsterdam) **341C–348C**, 1109 (2000).
[23] S. Berry *et al.,* Physica (Amsterdam) **282C–287C**, 2259 (1997).
[24] At low temperature (but still above the SMP temperature T_{cr}), the large barrier magnetization owing to small sample size obscures the observation of the small magnetization jump upon melting. Thus, at present we cannot resolve the melting jump below $T = 60$ K.
[25] M. Tinkham, *Introduction to Superconductivity* (McGraw-Hill, New York, 1996), 2nd ed.
[26] M. Nideröst *et al.,* Phys. Rev. Lett. **81**, 3231 (1998).